Stability of Internally Pressurized Conical Shells under Torsion

V. I. WEINGARTEN*
University of Southern California, Los Angeles, Calif.

An experimental investigation was made to determine the effect of internal pressure on the buckling stress of conical shells under torsion. The experimental results were compared with an analysis based on linear theory. It was found that no general interaction formula could be written for a pressurized conical shell under torsion and that an interaction curve must be computed for specific cases.

Nomenclature

E = modulus of elasticity
h = thickness of shell
l = slant length of cone
n = number of circumferential waves
p = internal hydrostatic pressure
p_e = critical external hydrostatic pressure defined by Eq. (2)
R_1 = radius of small end of truncated cone
R_2 = radius of large end of truncated cone
T = torque
Z = curvature parameter for cylinder $(1 - \nu^2)^{1/2}(L^2/Rh)$
α = semivertex angle of the cone
ν = Poisson's ratio
ρ_{av} = mean radius of curvature $= (R_1 + R_2)/2 \cos\alpha$
τ = maximum torsional stress $= (T/2\pi R_1^2 h)$
τ_{cr} = critical torsional stress given by Eq. (1)

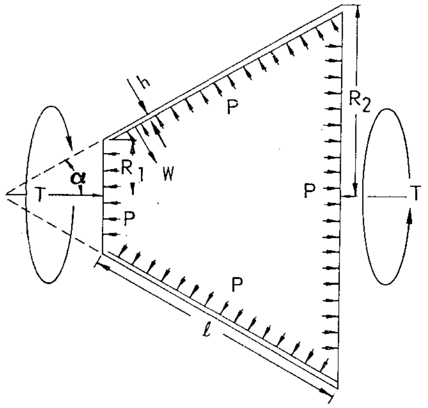

Fig. 1 Internally pressurized conical shell under torsion.

Introduction

AN analytical and experimental investigation on the stability of internally pressurized cylindrical shells under torsion was performed by the author and documented in Ref. 1. A similar investigation for conical shells is discussed in this paper.

A number of solutions for the buckling of cones under torsion can be found in Refs. 2–5. In Refs. 4 and 5, the solutions include the effects of internal or external pressures and axial compression, although numerical results are restricted to pure torsion in Ref. 4 and to torsion and external pressure in Ref. 5. In the present investigation, the analysis given in Ref. 5 is used to obtain numerical values of the critical torsional loads of selected internally pressurized conical shells (Fig. 1) for comparison with experimental results. Experimental results for unpressurized cones are also compared with the analysis given in Ref. 4. Unlike the investigation in Ref. 1 for cylinders, no simple expression for the interaction curve between torsion and internal pressure was found for conical shells. It appears that the interaction curve is a function of so many parameters that theoretical results must be obtained for each specific case.

Details of Experimental Investigation

The cones used in the experiments were made of Mylar polyester plastic. This material has been found to have the following approximate mechanical properties: a Young's modulus of 700,000 psi, Poisson's ratio of 0.3, and proportional limit and yield stresses of 6000 and 11,000 psi, respectively. All specimens had a large cross-sectional radius of 5 in. and various small radii. The semivertex angles of the cones tested were 20°, 30°, 45°, and 60°. The specimens were cut in the form of developed cones from flat sheets from the Mylar roll, formed on a mandrel with a $\frac{3}{4}$-in. lap joint, and then clamped in aluminum end plates having troughs that were filled with cerrobend, a low-melting-point alloy.

The Mylar cones were tested in the fixture shown in Fig. 2. Equal and opposite loads, monitored by a load cell, were applied by a cable to the ends of a loading beam attached to the upper plate. Internal pressure was provided by compressed air and measured with the use of a pressure transducer.

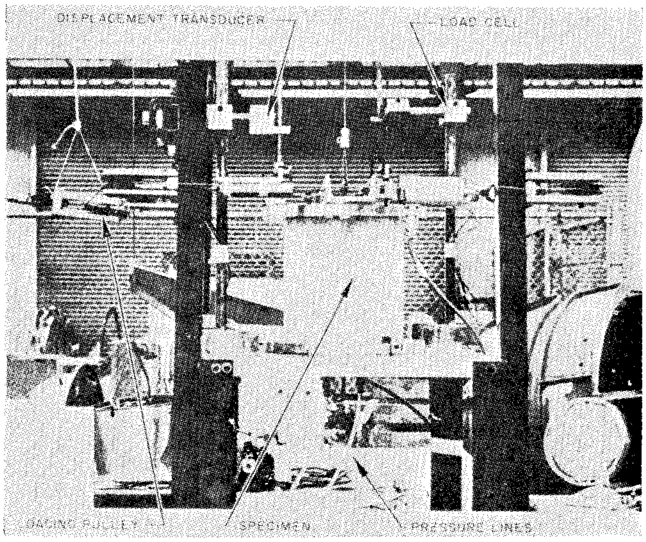

Fig. 2 Experimental test rig.

Received October 23, 1963; revision received June 19, 1964. The work reported herein was performed at the Space Technology Laboratories, Redondo Beach, Calif., under Contract No. AF 04(647)-619 and at the Aerospace Corporation, El Segundo, Calif. under Contract No. AF 04(695)-269.

* Assistant Professor of Civil Engineering; also consultant at Northrop Norair, Hawthorne, Calif. Member AIAA.

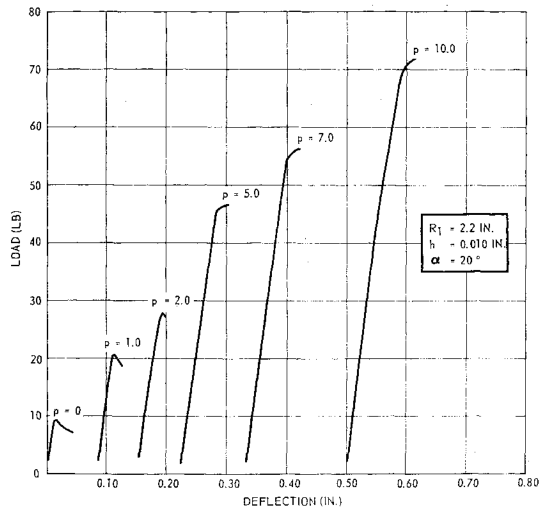

Fig. 3 Typical variation of load-deflection curve with pressure for a conical frustrum in torsion.

Measurements of angle of twist of the loaded end plate were obtained by means of two differential transformers. The output of the load cells and differential transformers was recorded by an X-Y plotter to yield a continuous record of torque vs angle of twist.

A set of typical torque-twist curves for a given cone under various values of internal pressure is shown in Fig. 3. At low pressures, buckling occurred with an N-shaped buckle pattern (Fig. 4) appearing suddenly and noisily. This phenomenon is represented in Fig. 3 by the sharp dropoff of load in the postbuckled region. As the pressure increased, the critical torque increased and the number of buckles grew. The shape of the buckles changed from the N-shaped to a pattern with about a 45° skew angle (Fig. 4). Instability no longer was accompanied by noise, and the torque no longer dropped, but actually increased in the postbuckling range. Buckling was determined by the point at which the torque-twist curve became nonlinear. Figure 4f shows the specimen at failure.

Because of the small variation of the properties of Mylar from roll to roll, the modulus of elasticity was determined for each test specimen by using the slope of the straight-line

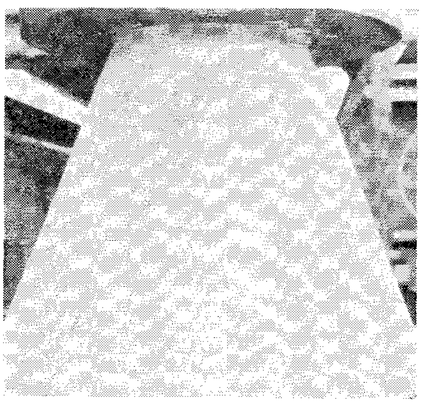

a) 0 psi

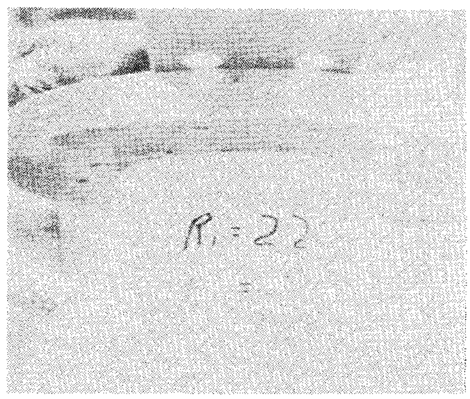

d) 5 psi

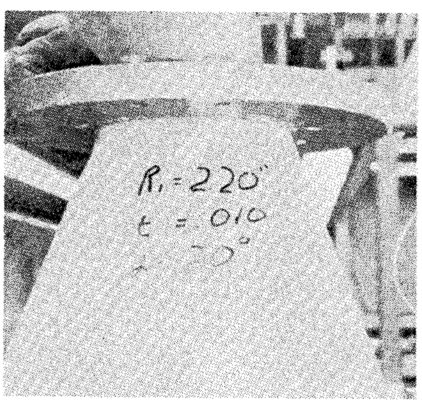

b) 1 psi

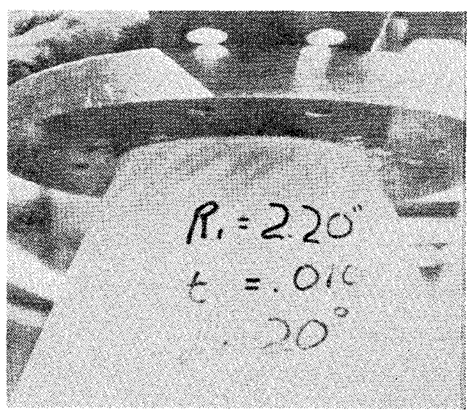

e) 7 psi

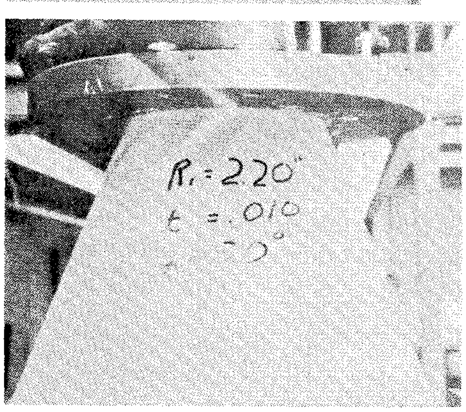

c) 2 psi

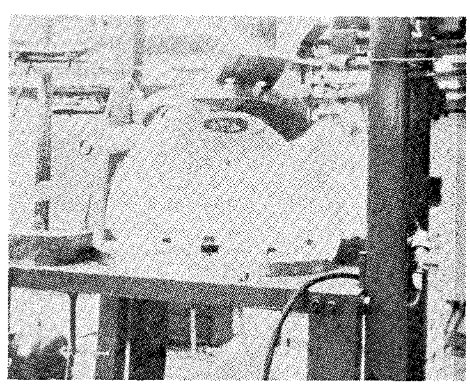

f) 10 psi

Fig. 4 Variation of buckling pattern with internal pressure.

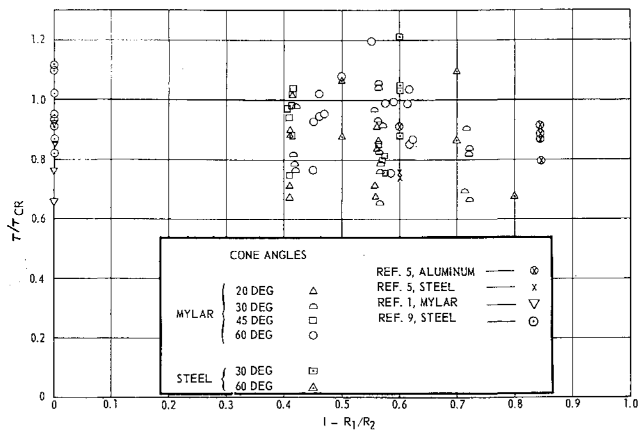

Fig. 5. Comparison of torsion test data with theory.

pattern of the curve of torque vs angle of twist obtained for each test specimen, in conjunction with the assumed value of Poisson's ratio.

Results and Discussion

Experimental critical shear stresses for unpressurized conical shells, designated τ, are given in Table 1 and are compared with the approximate theoretical predictions of Ref. 4, designated τ_{cr}, which may be written as

$$\frac{\tau_{cr}}{D/2R_1^2} = 16.8\left(\frac{h}{H}\right)^{1/2} \times \left(\left\{1 + \left[\frac{1}{2}\left(1 + \frac{R_2}{R_1}\right)\right]^{1/2} - \left[\frac{1}{2}\left(1 + \frac{R_2}{R_1}\right)\right]^{-1/2}\right\} \frac{R_1 \cos\alpha}{h}\right)^{5/4} \quad (1)$$

The results of Ref. 5 are almost identical to those of Ref. 4. A plot of these results is given in Fig. 5.

It is evident that there is a large scatter band for the cone data, the average being about 88% of the theoretical value with the extremes ranging from 67 to 122% of the theoretical value. It should be noted, however, that this scatter is comparable to that obtained for cylindrical shells. Thus, the comparison of theory and experiment for conical shells indicates that the recommendation of Ref. 4, that the theoretical value of critical shear stress (or critical torque) for conical shells be multiplied by the same reduction factor as is used for cylindrical shells, is valid.

Typical experimental results for the pressurized conical frustums investigated are given in Table 2. A complete tabulation of the experimental data is given in Ref. 10. Reference 10 is a preliminary report that lists all of the experimental data. The geometries were picked so that a large number of specimens with the same radius ratio but different thicknesses and angles could be studied. Theoretical data obtained with the use of the analysis of Ref. 5 are given in Table 3. The results were obtained with the aid of a digital computer by truncating the stability determinant of Ref. 5 and finding the lowest eigenvalue by matrix iteration. The size of the determinant was increased until the buckling coefficient converged. Convergence was very slow with an average of 21 terms being required in the deflection function for two significant figure convergence. As a check of the computer program, a number of test cases were computed. The computer results checked the values given in Ref. 5 and the results for cylinders given in Ref. 1. The values of p_e used in Tables 2 and 3 were computed from the approximate equation given in Ref. 6 as

$$p_e = 0.92E/[(l/\rho)(\rho/h)^{5/2}] \quad (2)$$

and τ_{cr} was computed from Eq. (1).

Table 1 Comparison of theory and experiment for unpressurized conical shells

h, in.	R_1, in.	R_2, in.	α, deg	$\tau \times 10^{-3}$, psi	τ/τ_{cr}	$E \times 10^{-6}$, psi
0.010[a]	4	10	30	11.650	1.050	30
0.010[a]	4	10	30	11.490	1.035	30
0.020[a]	4	10	30	32.400	1.219	30
0.020[a]	4	10	30	23.400	0.881	30
0.010[a]	2	10	60	14.300	0.680	30
0.010[a]	2	10	60	14.300	0.680	30
0.010[a]	3	10	60	10.800	0.867	30
0.010[a]	3	10	60	13.600	1.091	30
0.010[a]	5	10	60	8.390	1.068	30
0.010[a]	5	10	60	6.900	0.879	30
0.010	2.93	5	20	0.395	1.019	0.690
0.010	2.95	5	20	0.342	0.880	0.690
0.010	2.95	5	20	0.349	0.899	0.690
0.010	2.20	5	20	0.449	0.914	0.690
0.010	2.20	5	20	0.411	0.835	0.690
0.010	2.19	5	20	0.432	0.867	0.690
0.005	2.22	5	20	0.143	0.712	0.670
0.005	2.22	5	20	0.143	0.712	0.670
0.005	2.22	5	20	0.134	0.674	0.670
0.005	2.96	5	20	0.106	0.671	0.690
0.005	2.96	5	20	0.113	0.715	0.670
0.010	1.42	5	30	0.884	0.908	0.750
0.010	1.40	5	30	0.793	0.824	0.730
0.010	1.40	5	30	0.835	0.837	0.757
0.010	2.93	5	30	0.352	0.825	0.662
0.010	2.91	5	30	0.348	0.768	0.698
0.010	2.90	5	30	0.365	0.815	0.697
0.010	2.18	5	30	0.541	0.967	0.646
0.010	2.16	5	30	0.569	0.912	0.748
0.010	2.22	5	30	0.500	0.963	0.641
0.010	2.19	5	30	0.506	0.926	0.675
0.010	2.18	5	30	0.493	0.900	0.680
0.005	2.94	5	30	...	...	0.840
0.005	2.94	5	30	...	...	0.840
0.005	2.92	5	30	0.159	0.786	0.730
0.005	2.18	5	30	0.187	0.760	0.695
0.005	2.18	5	30	0.194	0.654	0.854
0.005	2.18	5	30	0.216	0.825	0.756
0.005	2.17	5	30	0.209	0.789	0.759
0.005	1.44	5	30	0.288	0.695	0.771
0.005	1.39	5	30	0.268	0.666	0.721
0.010	2.15	5	45	0.498	0.797	0.732
0.010	2.13	5	45	0.548	0.758	0.840
0.010	2.13	5	45	0.548	0.810	0.785
0.0075	2.92	5	45	0.344	1.036	0.720
0.010	2.97	5	45	0.423	0.938	0.690
0.010	2.94	5	45	0.465	1.011	0.700
0.010	2.93	5	45	0.439	0.880	0.758
0.005	2.19	5	45	0.225	0.855	0.746
0.005	2.97	5	45	0.173	0.964	0.746
0.005	2.96	5	45	0.151	0.743	0.746
0.005	2.95	5	45	0.202	0.984	0.746
0.010	1.92	5	60	0.590	1.037	0.700
0.010	1.92	5	60	0.484	0.850	0.700
0.010	1.90	5	60	0.500	0.865	0.700
0.010	1.21	5	60	...	...	0.700
0.010	2.50	5	60	0.478	1.073	0.700
0.010	2.14	5	60	0.507	0.989	0.700
0.010	2.07	5	60	0.518	0.992	0.690
0.010	1.94	5	60	0.551	0.989	0.690
0.010	2.76	5	60	0.381	0.928	0.700
0.010	2.71	5	60	0.435	1.019	0.700
0.010	2.71	5	60	0.392	0.944	0.690
0.010	2.67	5	60	0.401	0.953	0.700
0.005	2.76	5	60	0.126	0.765	0.670
0.005	2.25	5	60	0.235	1.196	0.670
0.005	2.08	5	60	0.161	0.759	0.670

[a] Preliminary tests on steel specimens which were reported in Ref. 9

Table 2 Typical experimental data for pressurized conical shells

h	R_1	E	p/p_e	τ/τ_{cr}	p/p_e	τ/τ_{cr}
0.010	2.20	690,000	0	0.914	27.059	3.264
(α = 20°)			0.966	1.166	28.992	3.351
			1.933	1.306	30.925	3.482
			2.899	1.428	32.858	3.613
			3.866	1.558	34.790	3.700
			4.832	1.654	36.723	3.830
			5.798	1.758	38.656	3.917
			6.765	1.828	40.589	4.048
			7.731	1.915	42.522	4.135
			8.698	2.011	44.454	4.265
			9.664	2.089	46.387	4.353
			10.630	2.159	48.320	4.440
			11.597	2.237	53.152	4.788
			12.563	2.316	57.984	5.005
			13.530	2.385	62.816	5.223
			14.496	2.464	67.648	5.484
			15.462	2.524	72.480	5.702
			17.395	2.655	77.312	5.946
			19.328	2.786	82.144	6.181
			21.261	2.960	86.976	6.398
			23.194	3.047	91.808	6.616
			25.126	3.134	96.640	6.790
0.010	2.20	690,000	0	0.835	27.059	2.977
(α = 20°)			0.966	1.062	28.992	3.090
			1.933	1.193	30.925	3.177
			2.899	1.306	32.858	3.221
			3.866	1.428	34.790	3.395
			4.832	1.515	36.724	3.526
			5.798	1.637	38.656	3.613
			6.765	1.671	40.589	3.726
			7.731	1.741	42.522	3.830
			8.698	1.811	44.454	3.917
			9.664	1.898	46.387	4.048
			10.630	1.958	48.320	4.135
			11.597	2.046	53.152	4.396
			12.563	2.107	57.984	4.614
			13.530	2.176	62.816	4.875
			14.496	2.246	67.648	5.092
			15.462	2.316	72.480	5.223
			17.395	2.437	77.312	5.441
			19.328	2.559	82.144	5.658
			21.261	2.646	86.976	5.832
			23.194	2.786	91.808	6.094
			25.126	2.890	96.640	6.267
0.010	2.13	840,000	0	0.758	13.074	2.527
(α = 45°)			0.594	0.935	14.263	2.622
			1.189	1.049	15.451	2.748
			1.783	1.188	16.640	2.906
			2.377	1.289	17.828	3.000
			2.971	1.377	19.017	3.095
			3.566	1.478	20.206	3.222
			4.160	1.560	21.394	3.316
			4.754	1.642	22.583	3.411
			5.349	1.712	23.771	3.538
			5.943	1.781	24.960	3.632
			6.537	1.851	26.148	3.664
			7.131	1.927	27.337	3.885
			7.726	1.984	28.525	4.011
			8.320	2.053	29.714	4.106
			8.914	2.085	32.685	4.359
			9.508	2.148	35.656	4.548
			10.697	2.293	38.628	4.738
			11.886	2.400	41.600	5.054

Theoretical and experimental results are compared in Fig. 6. It can be seen that theory and experiment check fairly well, with the experimental curve generally falling below the theoretical curve. The difference between theory and experiment can be attributed to a number of causes. Possible theoretical factors are insufficient convergence of the calculations, the use of membrane theory for the prebuckling stress state, and the use of classical small-deflection theory that assumes the shell retains its conical shape rather than a theory

Table 2 (Continued)

h	R_1	E	p/p_e	τ/τ_{cr}	p/p_e	τ/τ_{cr}
0.010	2.13	785,000	0	0.810	13.986	2.797
(α = 45°)			0.635	0.973	15.258	2.906
			1.271	1.108	16.529	3.041
			1.907	1.243	17.800	3.175
			2.543	1.331	19.072	3.297
			3.179	1.432	20.343	3.433
			3.814	1.527	21.615	3.581
			4.450	1.622	22.886	3.649
			5.086	1.703	24.158	3.784
			5.722	1.784	25.429	3.919
			6.357	1.865	26.701	4.020
			6.993	1.939	27.972	4.156
			7.629	2.027	29.244	4.223
			8.264	2.101	30.515	4.392
			8.900	2.169	31.787	4.460
			9.536	2.310	34.965	4.764
			10.172	2.365	38.144	5.068
			11.443	2.500	41.322	5.338
			12.715	2.635	44.501	5.608

Table 3 Computer data for pressurized conical frustums under torsion

α, deg	h, in.	R_1, in.	$E \times 10^{-6}$, psi	p/p_e	τ/τ_{cr}	n
20	0.010	2.22	0.690	0	1.05	9
20	0.010	2.22	0.690	10.63	2.26	13
20	0.010	2.22	0.690	30.92	3.85	14
20	0.010	2.22	0.690	48.32	4.98	14
20	0.010	2.22	0.690	67.64	6.22	13
20	0.010	2.22	0.690	96.64	8.16	13
20	0.010	2.95	0.690	0	0.98	12
20	0.010	2.95	0.690	0.82	1.26	13
20	0.010	2.95	0.690	4.10	1.96	15
20	0.010	2.95	0.690	9.03	2.68	16
20	0.010	2.95	0.690	11.50	3.00	16
20	0.010	2.95	0.690	19.71	3.97	16
20	0.010	2.95	0.690	29.57	5.06	16
20	0.010	2.95	0.690	49.28	7.14	16
20	0.010	2.95	0.690	73.92	9.64	16
20	0.010	2.95	0.690	82.14	10.45	16
20	0.005	2.22	0.670	0	0.99	12
20	0.005	2.22	0.670	5.61	1.84	16
20	0.005	2.22	0.670	28.06	2.41	18
20	0.005	2.22	0.670	50.51	3.56	17
20	0.005	2.22	0.670	84.18	5.39	17
20	0.005	2.22	0.670	134.68	7.74	15
20	0.005	2.22	0.670	202.02	10.75	14
20	0.005	2.22	0.670	258.14	13.19	14
30	0.010	2.91	0.678	0	0.99	13
30	0.010	2.91	0.678	2.54	1.72	15
30	0.010	2.91	0.678	10.17	3.04	16
30	0.010	2.91	0.678	21.62	4.63	16
30	0.010	2.91	0.678	30.53	5.77	16
30	0.010	2.91	0.678	41.34	7.13	16
30	0.010	2.91	0.678	60.42	9.51	15
30	0.010	1.42	0.750	0	0.98	9
30	0.010	1.42	0.750	2.226	1.29	10
30	0.010	1.42	0.750	6.678	1.62	11
30	0.010	1.42	0.750	9.645	1.78	11
30	0.010	1.42	0.750	14.839	2.04	10
45	0.010	2.13	0.785	0	0.99	11
45	0.010	2.13	0.785	5.34	1.99	13
45	0.010	2.13	0.785	10.69	2.63	13
45	0.010	2.13	0.785	15.45	3.13	13
45	0.010	2.13	0.785	24.96	4.06	13
45	0.010	2.13	0.785	41.60	5.50	13
60	0.010	1.92	0.700	0	1.01	10
60	0.010	1.92	0.700	6.15	2.15	11
60	0.010	1.92	0.700	12.31	2.91	11
60	0.010	1.92	0.700	18.47	3.59	11
60	0.010	1.92	0.700	27.09	4.45	11
60	0.010	1.92	0.700	39.40	5.64	11

such as used by Stein[7] and Fischer[8] for cylinders which considers the prebuckling change of shape of the shell. A possible experimental factor is the difference in boundary conditions between theory and experiment and yielding of the cone material near the small end as the pressure was increased.

The experimental results agree qualitatively with the simple interaction formula for a cylindrical shell under torsion and internal hydrostatic pressure[1] which can be written as

$$\left(\frac{\tau}{\tau_{cr}}\right)^2 = \left[1 + \frac{0.494}{Z^{1/2}}\frac{p}{p_e}\right]\left[1 + \frac{p}{p_e}\right] \qquad (3)$$

Results obtained for other loadings[9] indicate that the cone can, in some cases, be replaced by an equivalent cylindrical shell whose radius is some representative radius of curvature of the cone and whose length is equal to the slant length of the cone. If we were to use, say, the average radius of curvature of the cone, the curvature parameter Z could be written as

$$Z = \frac{2(R_2 - R_1)^2}{(R_2 + R_1)h}\frac{\cos\alpha}{\sin^2\alpha} \qquad (4)$$

Equations (3) and (4) then indicate that, for given value of p/p_e, (τ/τ_{cr}) should increase as R_1, h, and α increase (with R_2 const) which agrees with the trends shown by the experimental data as plotted in Figs. 7–9. The quantitative agreement between Eq. (3) and the experimental results is poor, however, for conical shells, although the agreement has been shown to be excellent for cylindrical shells in Ref. 1.

In addition to the critical stress parameter (τ/τ_{cr}), the number of circumferential waves at buckling was also computed and is listed in Table 3. It is interesting to note that the number of buckles for the conical frustrums did not increase greatly with increasing pressure. This agrees with the results for cylindrical shells given in Ref. 1.

Concluding Remarks

The stability of pressurized conical shells under torsion has been investigated experimentally, and the results have been found to be in very close agreement with those given by the theory of Ref. 5. It is found, however, that no general interaction formula, such as that given in Ref. 1 for pressur-

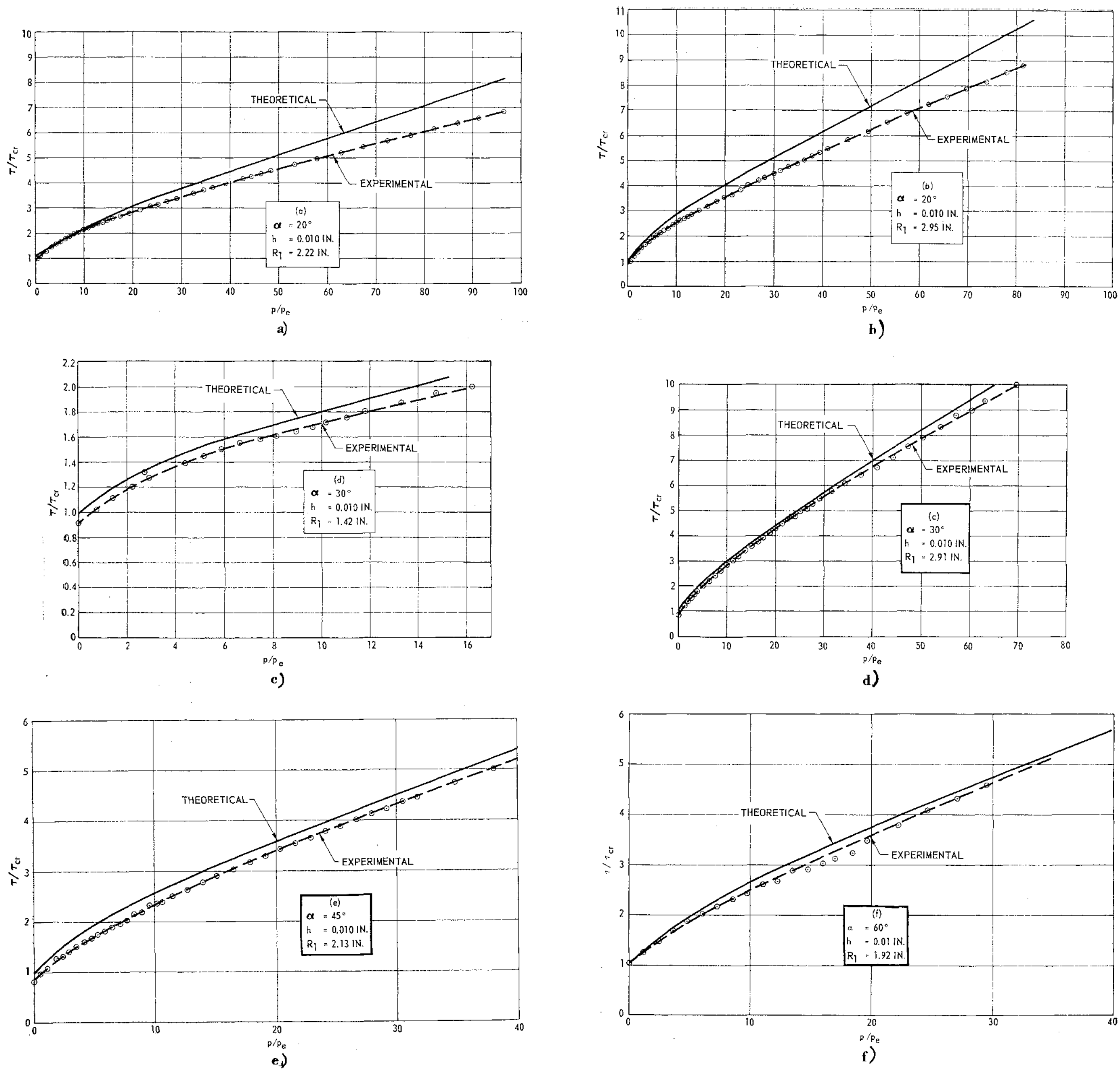

Fig. 6 Comparison of theoretical and experimental results for internally pressurized conical shells under torsion.

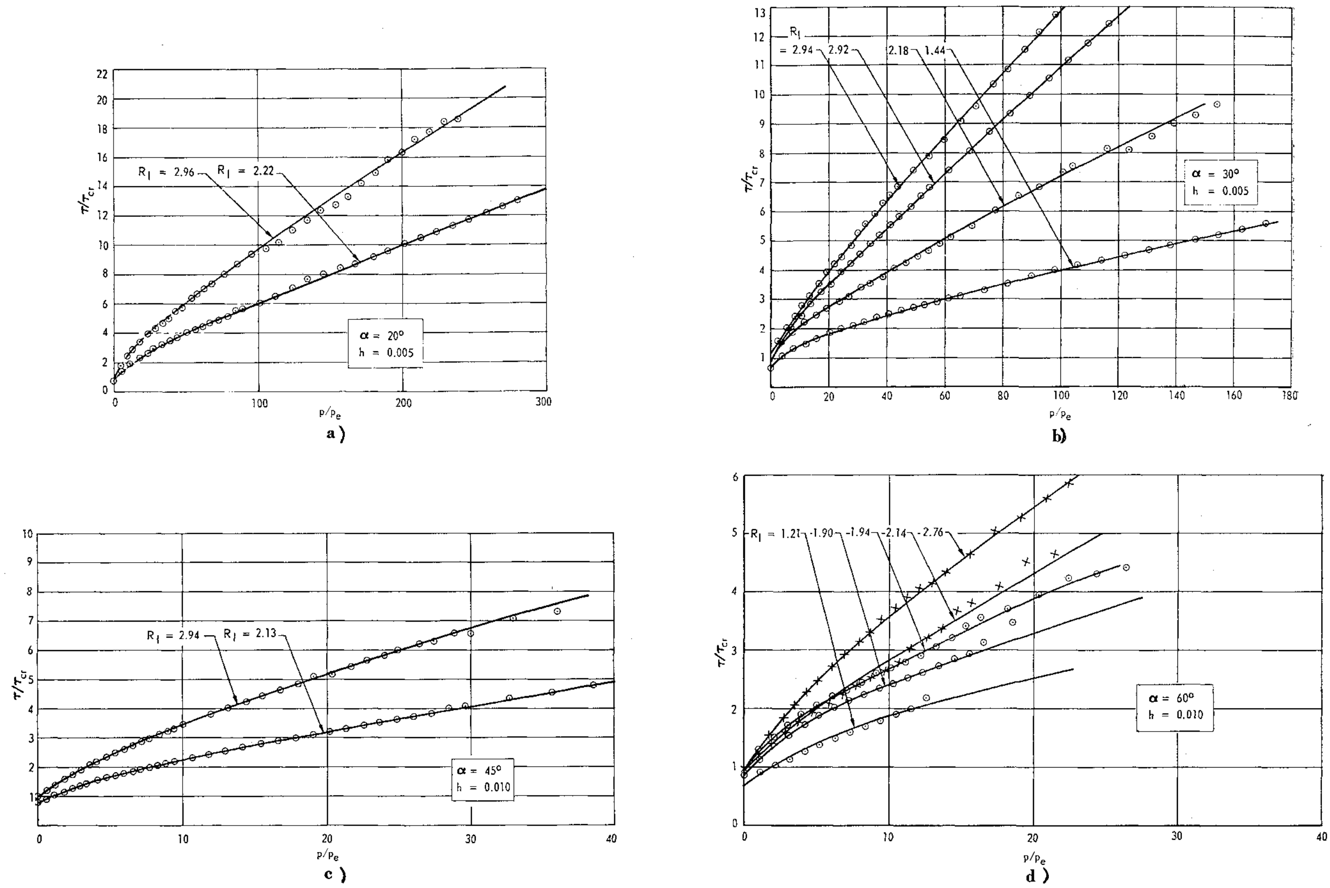

Fig. 7 Variation of critical shear stress with small radius.

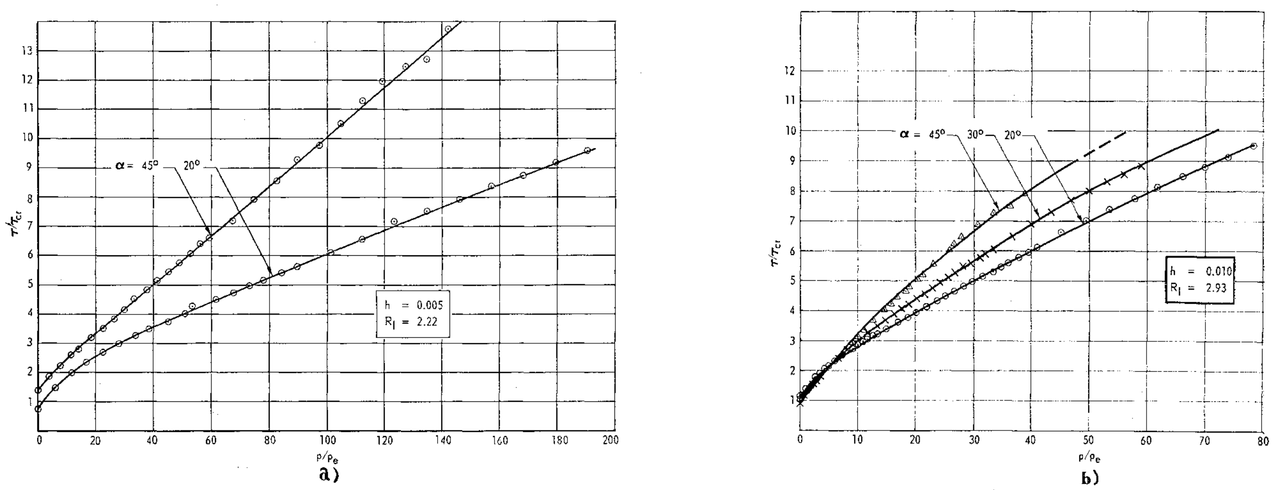

Fig. 8 Variation of critical shear stress with cone angle.

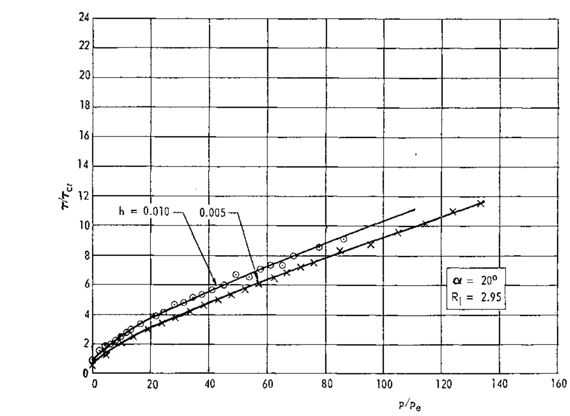

Fig. 9 Variation of critical shear stress with thickness.

ized cylinders under torsion, can be written for conical shells, so that the interaction curve must be computed for specific cases.

References

[1] Weingarten, V. I., "The effect of internal pressure and axial tension on the buckling of cylindrical shells under torsion," *Proceedings of the 4th U. S. National Congress of Applied Mechanics* (University of California Press, Berkeley, Calif. 1962), pp. 827–842.

[2] Pflüger, A., "Zur Stabilität der dünnen Kegelschale," Ingr.-Arch. **XIII**, 59–72 (1942).

[3] Mushtari, Kh. M. and Galimov, K. Z., *Non-Linear Theory of Thin Elastic Shells* (Academy of Sciences, USSR, Kazan Branch, 1957), pp. 300–304; transl. and available as NASA-TT-F62 (1961).

[4] Seide, P., "On the buckling of truncated conical shells in torsion," J. Appl. Mech. **29**, 320–328 (June 1962).

[5] Singer, J., Eckstein, A., and Baruch, M., "Buckling of conical shells under external pressure, torsion, and axial compression," Technion Research and Development Foundation, TAE Rept. 19, TR (Final) Contract AF61(052)-339 (September 1962).

[6] Seide, P., "On the buckling of truncated conical shells under uniform hydrostatic pressure," *Proceedings of the IUTAM Symposium on the Theory of Thin Elastic Shells* (North Holland Publishing Co., Amsterdam, Holland, 1960).

[7] Stein, M., "The effect on the buckling of perfect cylinders of pre-buckling deformations and stresses induced by edge support," *Collected Papers on Instability of Shell Structures—1962*, NASA TN D-1510 (December 1962), pp. 317–327.

[8] Fischer, G., "Über der Einfluss der gelenkigen Lagerung auf die Stabilität dünnwandiger Kreiszylinderschalen unter Axiallast und Innerdruct," Z. Flugwiss **11**, 111–119 (1963); transl. and available as Northrop Corp. Rept. NOR 64-80.

[9] Seide, P., Weingarten, V. I., and Morgan, D. J., "Final report on the development of design criteria for elastic stability of thin shell structure," Space Technology Labs., Rept. STL/TR-60-0000-19425, EM 10-26, Air Force Ballistic Missile Div./TR-61-7 (December 31, 1960).

[10] Weingarten, V. I., "Experimental investigation of the stability of internally pressurized conical shells under torsion," Aerospace Corp. Rept. TDR-269 (4560-40)-1 (1964).

OCTOBER 1964 AIAA JOURNAL VOL. 2, NO. 10

Nonlinear Response of Cylindrical Shells Subjected to Dynamic Axial Loads

Robert S. Roth* and Jerome M. Klosner†
Avco Corporation, Wilmington, Mass.

A study has been made to determine the dynamic instability of long, circular cylindrical shells having initial imperfections subjected to time-dependent axial edge loads. By using a nonlinear shell theory and including the radial inertia terms, equations of the Kármán-Tsien type were derived. Rather than attempt to solve the equations directly, an approximate four-term deflection function having time-dependent coefficients was assumed, and, by applying Hamilton's principle, a system of four coupled, second-order differential equations relating these coefficients was obtained. A numerical-integration scheme was used to solve these equations as a function of five parameters; namely, two initial imperfection parameters, two parameters governing the time-dependent geometrical configuration of the shell (equivalent to selecting the number of waves in the axial and circumferential directions), and the applied axial compressive load. A criterion for the dynamic buckling load of the cylinder has been established, and a study has been made of the magnitude of the critical loads on the shell as a function of the initial imperfections. The effect of applying a load for a short time has revealed that a significant increase in the dynamic buckling stress occurs as the time duration of loading decreases.

Nomenclature

$a_1(t) \ldots a_4(t)$	= coefficients of the assumed deflection shape [Eq. (11)]
c	= speed of sound in the material ($c^2 = E/\rho$)
d_1, d_2	= coefficients of the initial deflection shape
D	= bending stiffness [$D = Eh^3/12(1 - \nu^2)$]
E	= Young's modulus
$F(x, y)$	= Airy stress function
g	= average circumferential stress due to average circumferential inertia term [Eq. (13)]
$\bar{g}$	= nondimensional average circumferential stress $\bar{g} = (gR/Eh)$
h	= shell thickness
$\bar{I}$	= nondimensional impulse
$\bar{I}_B$	= nondimensional critical impulse
L	= shell length
m, n	= number of axial and circumferential waves, respectively
R	= mean shell radius
t	= time
T	= kinetic energy of the shell
u, v	= axial and circumferential radial displacements of the median surface, respectively
V_1, V_2, V_3	= extensional strain energy, bending strain energy, and potential of applied axial loads, respectively
w	= inward radial displacement of the median surface
$\bar{w}$	= initial inward radial displacement
w^*	= total inward radial displacement ($w^* = w + \bar{w}$)
x, y	= axial and circumferential coordinates on median surface of shell, respectively
α	= geometrical parameter ($\alpha = \lambda_y^2/\pi^2 Rh$)
β	= geometrical parameter ($\beta = \lambda_y/\lambda_x$)
$\gamma_{xy}, \epsilon_x, \epsilon_y$	= median surface shear, axial, and circumferential strains, respectively
ϵ	= unit end shortening of shell
λ_x, λ_y	= half-wavelengths in the axial and circumferential directions, respectively
ν	= Poisson's ratio
ρ	= mass density of shell material
σ	= applied average axial compressive stress
$\bar{\sigma}$	= nondimensional applied average compressive stress $\bar{\sigma} = (\sigma R/Eh)$

Presented as Preprint 64-76 at the AIAA Aerospace Sciences Meeting, New York, January 20–22, 1964; revision received July 1, 1964. This study was sponsored in part by the U. S. Air Force under Contract AF04(694)-239 with the Avco Corporation.

* Staff Scientist. Member AIAA.

† Consultant; also Associate Professor of Applied Mechanics, Polytechnic Institute of Brooklyn, Brooklyn, N. Y. Member AIAA.